

PHYSICAL REVIEW B

CONDENSED MATTER

THIRD SERIES, VOLUME 37, NUMBER 12

15 APRIL 1988-II

Effect of Sm valence changes on photoemission spectra

M. L. denBoer and C. L. Chang

Hunter College of the City University of New York, 695 Park Avenue, New York, New York 10021

S. Horn

New York University, 4 Washington Place, New York, New York 10003

V. Murgai

Boston University, 590 Commonwealth Avenue, Boston, Massachusetts 00215

(Received 6 August 1987)

We have used low-energy ($h\nu=17-45$ eV) photoemission to study thin films of Sm evaporated on Nb. We find that Sm evaporated onto a room-temperature Nb substrate is initially entirely divalent. On a time scale of the order of 50 min at room temperature a valence transition to mixed-valent or trivalent Sm occurs. This is accompanied by dramatic changes in the photoemission spectra, including a large increase in the total yield of photoelectrons and the appearance of a series of new constant-kinetic-energy peaks. The photon-energy dependence of these peaks indicates that they are due to Auger recombination of the Sm $5p$ level. We also observe a $5p \rightarrow 5d$ resonance in Sm for the first time. The underlying cause of these effects appears to be an ordering transition in the Sm film, which changes the Sm $5d$ occupancy and increases the resonance amplitude. This mechanism is evidently a very sensitive indicator of a Sm valence change.

INTRODUCTION

Certain rare-earth ions may exist in an intermediate valence state.¹ For Sm, this is a mixture of the configurations $[\text{Xe}]4f^6s^2$ and $[\text{Xe}]4f^55d^16s^2$, in which the Sm is, respectively, divalent and trivalent, as the f electron is highly localized and participates minimally in bonding. As these configurations are nearly energy degenerate, either may be preferred in the ground state depending on the chemical environment. Bremsstrahlung isochromat spectroscopy indicates² that in fully coordinated bulk Sm the f^6 configuration is 0.46 eV above the Fermi level. However, photoemission has shown³ that the surface Sm atoms are divalent due to the reduced coordination number. A surface shift brings the f^6 configuration below E_F . The valence of Sm films was studied by Fäldt and Myers⁴ with x-ray photoemission spectroscopy (XPS); they found that the Sm valence depends on the degree of order in the layer, its thickness, and the substrate.

We have studied Sm evaporated on Nb substrates with much lower photon energies, 15 to 45 eV, than previous work. We find dramatic qualitative and quantitative

changes in the energy distribution and yield of photoelectrons from the Sm films, coincident with changes in the Sm valence. As initially laid down, the Sm is entirely divalent, and over a period of time a portion becomes mixed valent or trivalent. This transition is indicated by the appearance of a trivalent photopeak and is associated with a large increase in Auger-electron emission evidently based on the Sm $5p$ core level as indicated by its photon-energy dependence. Accompanying the valence transition is a large increase in photoyield at low kinetic energies and other changes in the spectrum, which we only partly understand. We also measure, for the first time in Sm, a $5p \rightarrow 5d$ resonance which is evidently sensitive to the occupancy of the Sm $5d$ states. This resonance appears similar to one observed in Yb and Eu.⁵

Experiments were carried out in an ultrahigh-vacuum chamber with a base pressure of about 1×10^{-10} Torr. Sm of 99.99% purity was evaporated onto Nb foil substrates; sample cleanliness was monitored by Auger-electron spectroscopy (AES) using a commercial single-pass cylindrical mirror analyzer with a coaxial electron gun and by low-energy photoemission. Before each evaporation the Nb was heated to above 2000°C to remove

adsorbed species and previously evaporated Sm. AES then showed only Nb and traces of C and O. As this high-temperature flashing eventually recrystallizes the Nb,⁶ it is likely that our substrate consisted largely of (110) facets. The Sm was evaporated from a resistively heated tungsten basket. During this process the pressure rose typically to 2×10^{-9} Torr. Although the amount deposited was not directly monitored, it could be indirectly determined by AES immediately after evaporation. After deposition of small amounts of Sm by using lower evaporation pressures and shorter times, peaks due to the Nb substrate were still evident in the spectrum. Slightly higher evaporation pressure and longer evaporation time eliminated these peaks. Given the mean free path of the relevant Nb Auger electrons, we believe the Sm was at least a few monolayers thick. No traces of common contaminants such as C and O were evident on any of the films studied.

Photons were obtained from the vacuum-ultraviolet ring of the National Synchrotron Light Source at Brookhaven National Laboratory. We used the Howells-type plane grating monochromator⁷ at line U7, which has a typical resolving power ($E/\Delta E$) of 100 in range 1, which extends from about 14 to 45 eV. The photoelectrons were measured by an angle-resolving 50-mm 150° sector analyzer operated with a fixed pass energy of 20 eV for an energy resolution of about 0.2 eV. Changing the incident angle of the photon beam on the sample or the takeoff angle of the analyzer had little effect on the measured spectra apart from small amplitude changes. All measurements reported here were taken with the photons incident at $\sim 40^\circ$ to the surface normal and the

analyzer $\sim 20^\circ$ from the surface normal, so that the angle between the incident light and the emitted electrons was $\sim 60^\circ$.

RESULTS

Curve *a* of Fig. 1 shows the electron energy distribution curve (EDC) of a clean Sm sample taken with 30-eV photons about 2 min after deposition. Peak 1 is primarily due to the $4f^5$ final state resulting from the ionization of divalent Sm and has a tail due to inelastically scattered electrons. Some emission from the broad $6s$ band is also expected in this energy range. There is no evidence of a $4f^4$ final state, which would be expected if trivalent Sm were present. Also apparent in this spectrum is a peak, 4, at about 5 eV, which is a constant-kinetic-energy feature as it does not shift with photon energy. Near zero kinetic energy there is a rise in intensity due to secondary electrons. After 50 min there is a complete change in the character of the EDC, as shown in curve *b* of Fig. 1. A pronounced new peak, 3, appears at a measured constant kinetic energy of ~ 12 eV. A series of small peaks, 2, due to trivalent Sm emerge above an increased tail of lower-kinetic-energy electrons below the $4f^5$ final-state peak. The spectrum continues to change with time—more peaks appear at still lower kinetic energy and there is a large increase in the total yield.

The various stages the Sm EDC's undergo do not change from one evaporation to another. In the case described above, the change from curve *a* to curve *b* (Fig. 1) occurred within 2 min (the time it took to obtain the spectrum), 50 min after deposition, but in other samples

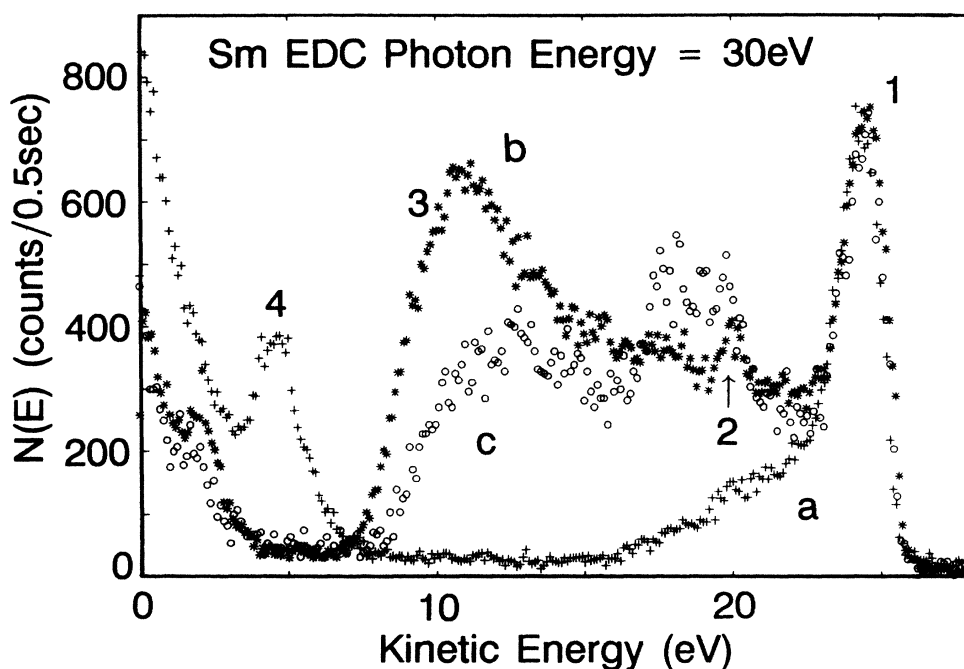


FIG. 1. Energy distribution curve of Sm films at 30 eV photon energy: (a) as initially deposited; (b) after 50 min; (c) a clean film exposed to 10 L of oxygen. The prominent peak 1 is due to Sm^{2+} and the presence of Sm^{3+} is indicated by the appearance of peak 2. Other features are described in the text.

the change sometimes occurred more gradually. However, whenever we started with a clean sample showing only Sm^{2+} , it went through the sequence of events described above, although the detailed shape and the time elapsed between each change varied. In Fig. 2(a), we show 30-eV photon-energy EDC's taken at the indicated times after deposition. In order to enhance detail in plots taken early in the evolution of the sample, the data are normalized to the same overall amplitude, resulting in a compression of the later figures. The extent of the compression, and thus the magnitude of the increase in low-energy yield with time, can be estimated by noting that the measured amplitude of the Sm^{2+} peak (peak 1) remains roughly constant at all times. Also apparent, in Fig. 2(a), is the growth in yield of electrons with kinetic energy between 18 and 22 eV, just below the Sm^{2+} peak. This growth merges with a rapidly rising peak, 3, which initially is at ~ 12 eV and shifts with time, as indicated by the dotted line, to 11 eV. The small peak, 4, at 6 eV shifts to lower energy and becomes less distinct. Also evident is an effect resembling a low-energy cutoff, marked by the dashed line, initially at about 14 eV, which moves to lower kinetic energy and becomes more distinct with time. The time evolution of the photoyield as a function of time is illustrated in Fig. 2(b). The amplitude initially

increases rapidly and saturates about 2 h after evaporation. The spectra reach a steady state after about 2 h. Contamination is seen only after several additional hours.

Figure 3 illustrates the photon-energy dependence of the features seen in the steady state. In Fig. 3(a), we plot a number of spectra taken with photon energies between 16 and 27 eV. As the energy dependence of the incident flux of this monochromator is not well known, these plots are normalized to constant Sm^{2+} peak amplitude. There is clearly a dramatic increase in electron yield at about $h\nu = 20$ eV, where the 11-eV peak becomes more distinct. This photon-energy dependence is also illustrated in Fig. 3(b), which plots the integrated intensity between 0 and 8 eV kinetic energy normalized to the divalent peak as a function of photon energy. The rapid rise at 20 eV looks much like a threshold effect, and is followed by a slow decrease in yield.

We stress that the effects discussed above do not appear to be related to surface contamination. Throughout these measurements the samples remained free of contaminants to which AES and low-energy photoemission are sensitive. In particular, there was no trace of C or O. Deliberately exposing a newly evaporated sample to O_2 did not produce the effects described above. Curve *c* of Fig. 1 shows the spectrum of Sm after exposure to 10 L (1

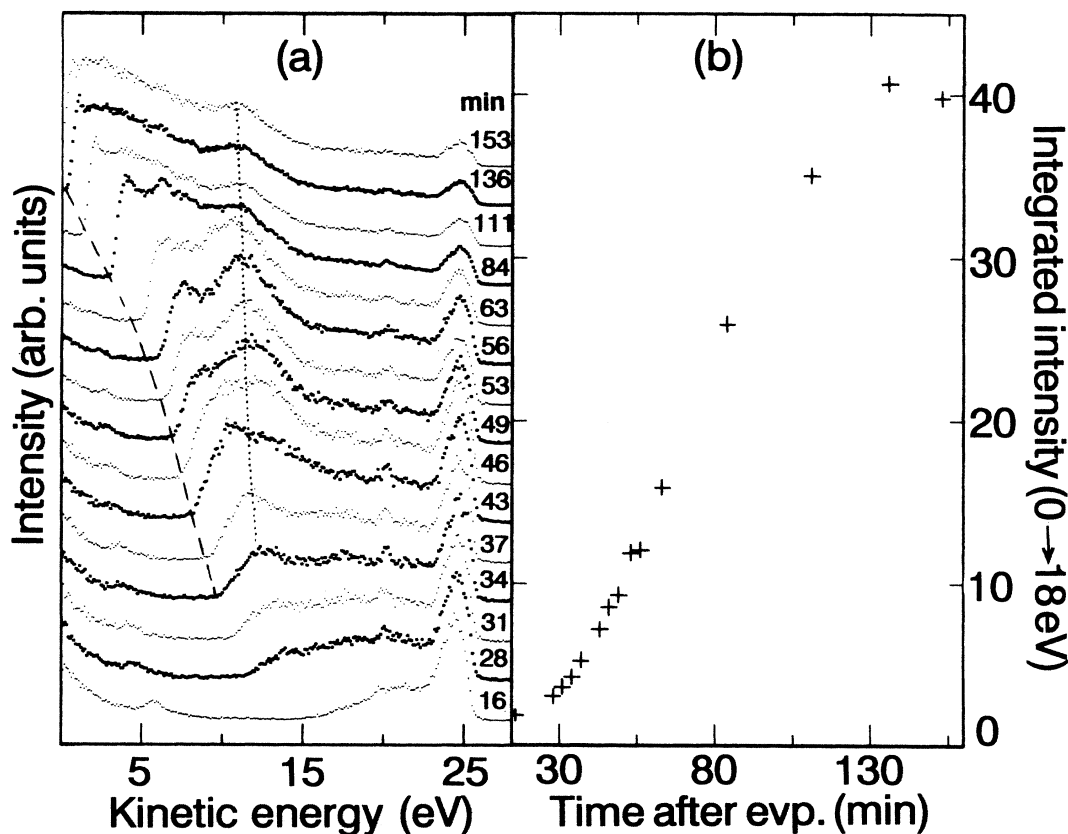


FIG. 2. Time evolution of the Sm photoemission features. (a) Energy distribution curves at 30 eV photon energy measured at times in minutes as indicated after sample deposition. The vertical scale is normalized to the maximum in each spectrum and the dashed and dotted lines are drawn to emphasize trends, as described in the text. (b) Integrated yield from 0 to 18 eV kinetic energy, plotted as a function of time after deposition, showing the large increase in total yield within 2 h.

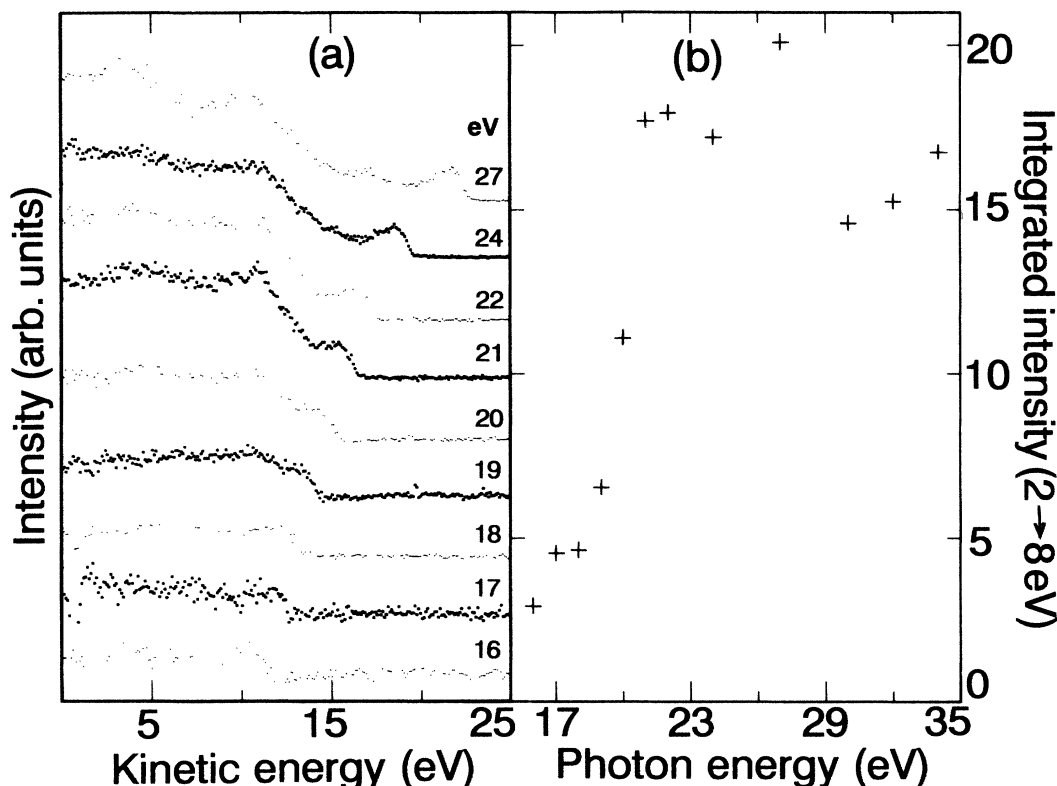


FIG. 3. Energy dependence of the Sm photoemission features: (a) Energy distribution curves of deposited Sm in the terminal stage of development, taken at various photon energies in eV as indicated. (b) Low-energy (2 to 8 eV) yield plotted as a function of incident photon energy, showing a threshold at about 19 eV.

$L = 1$ langmuir $= 10^{-6}$ Torr sec) of O_2 . This has the characteristic oxygen $2p$ peak ~ 7 eV below the Fermi level, which is absent in films not intentionally exposed to O_2 . Oxygen was also evident in the Auger spectrum of this sample. The primary features of our results can be summarized as follows: (i) a transition from divalent Sm to mixed-valent or trivalent Sm as deduced from the emergence of a $4f^4$ final-state peak, (ii) the appearance of constant-kinetic-energy features such as peak 3 which are not present when the Sm is purely divalent, (iii) an increase in the secondary electron yield accompanying the divalent to mixed-valent transition, and (iv) an increase in the secondary electron yield on going through the $5p$ threshold.

DISCUSSION

The dramatic changes in the photoemission from Sm must be indicative of extensive modifications of the surface Sm electronic structure. Though the data presented here are inadequate to completely characterize these changes, a number of conclusions can be drawn. Any explanation must include the fact that the changes in the photoemission spectra are clearly associated with a valence transition in Sm. In the following, we discuss the origin of the 11-eV constant-kinetic-energy feature (peak 3) and the photoyield increases accompanying the valence

transition. We then present a framework within which we discuss the photoyield changes, and finally we compare our results to measurements of Sm overlayers on other substrates.

Peak 3 appears simultaneously with the development of the $4f^4$ final-state peaks characteristic of mixed-valent or trivalent Sm. As peak 3 is at a constant kinetic energy, it must be due to an Auger process. Its kinetic energy and photon-energy threshold of about 20 eV imply it is due to Auger recombination of the Sm $5p$ core level, which has a binding energy of about 19.5 eV.¹⁰ The corresponding direct $Sm^{3+} 5p$ photopeak also expected would emerge with only about 5 eV of kinetic energy, too little to be distinguished from the secondaries. There are a number of possible two-hole final states produced by Auger recombination of an initial $5p$ hole. Labeled by the atomic notation of the holes, these are (ff) , (df) , (sf) , (dd) , and (ss) . The latter two possibilities may be excluded because of the sharpness of peak 3. Energy considerations eliminate others: The kinetic energy of Auger electrons is, following Mathews,⁸

$$E_{\text{Auger}}(5p, x, y) = E(5p) - E(x) - E(y) - \delta,$$

where $E(5p)$ is the energy of the $5p$ core hole and $E(x)$ and $E(y)$ are the energies of the levels in which vacancies are created. δ is a correction factor which includes final-state coupling terms and relaxation effects; for the

present case, it is about 5.5 eV.⁹ For Sm, $E(5p_{3/2})$ is about 19.5 eV,¹⁰ and Fig. 1 shows $E(f)$ in trivalent Sm is 5 eV below the Fermi level. This gives an estimate of $E_{\text{Auger}}(5p, x, y)$ of less than 4 eV above E_F if x and y are both f states. The kinetic energy measured is found by subtracting the work function. Figure 1 shows that an electron ejected from the Fermi level by a 30-eV photon emerges with a kinetic energy in the vacuum of about 25.5 eV. Thus an electron with 4 eV of energy relative to E_F will not be observed. Peak 3, which is at a substantially higher energy above E_F , must therefore be based on a (df) or (sf) process.

It is necessary to explain why this Auger process is only observed as the Sm valence changes. We believe that this is because, to the extent to which we can speak of separate $6s$ and $5d$ bands, the formation of Sm^{3+} promotes an electron to the Sm $5d$ band, which is unoccupied in Sm^{2+} . This has two effects. It allows the highly probable (df) Coster-Kronig Auger process of a $5p$ hole decaying into $5d$ and $4f$ holes to occur, increasing the contribution of this Auger recombination to peak 3. Moreover, the valence change also increases the amplitude of a resonant photoabsorption process, analogous to the giant $4f \rightarrow 4d$ resonance observed in all the rare earths.¹¹ Although there is more than one way to think of the giant resonance process, perhaps the simplest and physically most appealing comes from the time-dependent local density approximation.¹² The $4d$ shell oscillates in response to the external (electromagnetic) field. Below resonance, the shell oscillates in phase with the external field so that the induced field screens the external field at radial distances inside the $4d$ -shell charge radius and enhances (or antiscreens) it beyond this radius. At the resonance position, the field thus induced oscillates 90° out of phase with the driving field and produces a peak in the $4d$ absorption. Above the resonance, the situation is reversed: the induced field is out of phase with the external field and the screening and antiscreening characteristics switch. Because the radial wave function of rare-earth $4f$ levels is very similar to the $4d$, it contributes to the polarization giving rise to the large increase in cross section. A $5p \rightarrow 5d$ resonance occurs in the same way. Calculations¹³ show the $4f \rightarrow 4d$ resonance is larger for trivalent Sm than divalent Sm. We suggest the same is true for the $5p \rightarrow 5d$ resonance. It is therefore appropriate to normalize the EDC's to the divalent Sm peak as a function of photon energy, which assumes that the divalent cross section does not change greatly with photon energy. Note that the total low-energy cross section as a function of energy reaches a maximum near the $5p_{3/2}$ binding energy and has a shape consistent with the shape of resonant functions. One higher point at $h\nu = 27$ eV may indicate the presence of a $5p_{1/2}$ resonance threshold.

Although a more thorough investigation of the changes in photoyield is required, we offer here a qualitative preliminary interpretation. The Sm as initially deposited is divalent and probably disordered, since as we discuss further below, Fäldt and Myers⁴ have found that ordered monolayers of Sm on various substrates are mixed valent. This structure may be visualized as an ir-

regular overlayer with an average thickness of a few atoms on the Nb substrate. In this configuration there will be few secondary electrons, as most primary electrons will pass through very little material as they leave the solid. After a period of time a Sm^{3+} peak appears, indicating a Sm valence increase to mixed valence or trivalence and a corresponding nonzero $5d$ -band occupancy. In fact, there is a general tendency for ordered layers of Sm to have a higher valence than disordered layers.⁴ Therefore we conclude that the deposited Sm has annealed at room temperature sufficiently to order the Sm, beginning with a layer of Sm atoms adjacent to the ordered Nb substrate. Our observations show that this ordering may occur very suddenly after a relatively long period of quiescence, suggesting a nucleation and growth mechanism. The ordered structure must be a configuration with lower free energy but with a formation barrier. Once ordering begins locally, the barrier height is reduced and ordering spreads rapidly throughout the Sm-Nb interfacial region. Note that there is a huge volume collapse associated with the divalent to trivalent transition—the ionic radius of Sm^{3+} is 0.18 Å smaller than Sm^{2+} . We conceive of the disorder-order transition as being driven by this volume collapse, which will extensively rearrange all the affected orbitals.

Surface ordering affects the photoelectric yield in several ways. The atoms in the ordered region, due to their higher valence, experience a larger $5p \rightarrow 5d$ resonance as mentioned above, causing an increase in the photoabsorption cross section. Incident photons normally deposit only a small proportion of their energy in the surface region to which photoemission is sensitive, as the photon absorption length is much longer than the electron mean free path. The resonant enhancement of the cross section causes this proportion to increase, resulting in an increase of the total secondary electron yield. The increased probability of ionization of the $5p$ levels also causes an increase in the yield of the corresponding Auger electrons. As the ordering continues from the substrate out to the surface, the Auger electrons emitted must pass through more material as they leave the solid and will suffer more inelastic losses, producing the observed growing inelastic tail of low-energy secondary electrons. Additionally, the increasing proportion of mixed or trivalent Sm continues to increase the total photoabsorption cross section and the total electron yield. However, the mean free path λ of the low-energy Auger electrons produced is much longer than that of the ~ 20 eV f^6 photoelectrons, because of the steep increase in λ with decreasing energy below 30 eV,¹⁴ and therefore the measured Auger yield will be much larger than the corresponding photopeak.

The properties of Sm films have been extensively studied by other workers, especially Fäldt and Myers,⁴ using both XPS and low-energy electron diffraction (LEED). As mentioned, they have found that the Sm valence depends on the degree of order in the layer, its thickness, and the substrate. Their LEED results indicated that Sm deposited on the Al(001) surface⁴ at room temperature did not produce an ordered overlayer—annealing to $\sim 150^\circ\text{C}$ was required. At the photon energy used (Al

$K\alpha$ at 1540 eV) they were unable to observe the dramatic changes in photoemission properties evident at the low energies used here. They found isolated Sm atoms were equally mixed valent on both the (100) and (111) surfaces of Al while ordered layers were trivalent. We find, in contrast, that on Nb disordered Sm is divalent like the isolated atom, and even layers we believe to be ordered are mixed valent, suggesting perhaps the Sm-Sm or Sm-Nb interaction is weaker than the Sm-Al interaction. In this respect, surprisingly, Nb seems to behave like Cu(001) and Si(001). On both surfaces, Fäldt and Myers⁴ found that isolated atoms were divalent and ordered layers mixed valent or trivalent.

Several observations show the observed valence and associated changes in the Sm layer are not simply due to contamination, including the suddenness of the transition and the fact that AES shows that none of the most common impurities, such as C, N, or O, are present. Hydrogen absorption is a possibility, as the background gas in the measurement chamber was mostly H_2 . However, we observed no correlation between the background pressure, which varied by as much as a factor of 2 between different runs, and the time required for the sample transformation. Moreover, as described above, the yield changes are more easily understood assuming changes proceed outward from the substrate to the surface, rather than proceeding inward from the surface to the substrate, as changes due to an absorbant would.

Although the above discussion adequately describes the basic processes occurring on the Sm surface, several questions remain. The low-energy constant-kinetic-energy peak, 4, of Fig. 1 must be an Auger feature. However, it is too narrow to be a candidate for any of the obvious transitions, and its shift to lower kinetic energy with time and eventual disappearance are also mysterious. The cause of the changing low-energy cutoff suggested by Fig. 2 is also unknown.

CONCLUSIONS

We have observed a room-temperature valence transition of Sm from divalent to mixed valent or trivalent. The dramatic changes in the photoabsorption cross section and yield characteristics observed in our Sm films are a fascinating example of the effect of a change of physical structure on the electronic properties of a system. The $5p \rightarrow 5d$ resonance in the rare-earth metals, which has only been previously identified unambiguously in Yb and Eu,⁵ merits systematic study throughout the rare-earth series. This should form an interesting contrast to the better-known $4d \rightarrow 4f$ "giant resonance." The resonance properties should be significantly affected by the increasing hybridization of the $5d$ band with the $4f$ and $6s$ states from left to right in the rare-earth series. The ordering properties of the Sm layers are interesting and demand further study by other techniques. Finally, the electronic transition observed here may be of great value in the characterization of Sm overlayers. If our interpretation is correct, the abrupt turning on of the resonance caused by the Sm valence change is an extremely sensitive indicator of the formation of an ordered overlayer. Similar effects should occur in all unstable valent rare-earth-based compounds (except Ce).

ACKNOWLEDGMENTS

This work was supported in part by the National Science Foundation under Grant No. DMR-8521561 and by the U.S. Department of Energy (DOE) under Grant No. DE-FG02-85ER45195. A part of this work was carried out at the National Synchrotron Light Source at Brookhaven National Laboratory, which is supported by the U.S. DOE Divisions of Materials Sciences and Chemical Sciences through Contract No. DE-AC02-76CH00016. We appreciate many valuable discussions with A. Zangwill.

¹J. M. Lawrence, P. S. Riseborough, and R. D. Parks, Rep. Prog. Phys. **44**, 1 (1981).

²J. K. Lang, Y. Baer, and P. A. Cox, J. Phys. F **11**, 121 (1981).

³G. K. Wertheim and G. Crecelius, Phys. Rev. Lett. **40**, 813 (1978); J. W. Allen, L. I. Johansson, R. S. Bauer, I. Lindau, and S. B. M. Hagström, *ibid.* **41**, 1499 (1978); F. Gerken, A. S. Flodström, J. Barth, L. I. Johansson, and C. Kunz, Phys. Scr. **32**, 43 (1985).

⁴Sm on Al(111): Å. Fäldt and H. P. Myers, Phys. Rev. B **34**, 6675 (1986); Sm on Al(001): *ibid.* **30**, 5481 (1984); Sm on Al(110): Solid State Commun. **48**, 253 (1983); Sm on Cu(001): Phys. Rev. Lett. **52**, 1315 (1984); Sm on Si(001): Phys. Rev. B **33**, 1424 (1986).

⁵G. Rossi and A. Barski, Phys. Rev. B **32**, 5492 (1985); Solid State Commun. **57**, 277 (1986).

⁶M. W. Ruckman, V. Murgai, and Myron Strongin, Phys. Rev. B **34**, 6759 (1986).

⁷M. R. Howells, Nucl. Instrum. Methods **177**, 127 (1980).

⁸J. A. D. Mathews, Surf. Sci. **89**, 596 (1979).

⁹See Ref. 2 and J. F. Herbst, R. E. Watson, and J. W. Wilkins, Phys. Rev. B **17**, 3089 (1978).

¹⁰See A. Franciosi, J. H. Weaver, P. Perfetti, A. D. Katnani, and G. Margaritondo, Solid State Commun. **47**, 427 (1983), and references cited therein. Our EDC's at higher photon energies are consistent with these results.

¹¹F. Gerken, J. Barth, and C. Kunz, in *X-Ray and Atomic Inner-Shell Physics (University of Oregon, Eugene, Oregon)*, Proceedings of the International Conference on X-Ray and Atomic Inner-Shell Physics—1982, AIP Conf. Proc. No. 94, edited by B. Crasemann (AIP, New York, 1982).

¹²A. Zangwill and P. Soven, Phys. Rev. Lett. **45**, 204 (1980).

¹³A. Zangwill, in *Giant Resonances in Atoms, Molecules, and Solids*, edited by R. Karnatak, J.-M. Esteve, and J. P. Connerade (Plenum, New York, 1987), p. 319.

¹⁴M. P. Seah and W. A. Dench, Surf. Interface Anal. **1**, 2 (1979); C. D. Wagner, L. E. Davis, and W. M. Riggs, *ibid.* **2**, 53 (1980).